

# Performance Analysis of Poisson-Voronoi Tessellated Random Cellular Networks Using Markov Chains

Xiaohu Ge\*, Bin Yang\*, Junliang Ye\*, Guoqiang Mao<sup>†</sup>, Qiang Li\*,

\*Dept. Electronics & Information Engineering, Huazhong University of Science & Technology, Wuhan, China

Email: {xhge, yangbin, m201271707, qli\_patrick}@mail.hust.edu.cn

<sup>†</sup> School of Computing and Communication, University of Technology Sydney, Australia

Email: g.mao@ieee.org

**Abstract**—Compared with the conventional hexagonal cellular network structure, Poisson-Voronoi tessellated (PVT) random cellular network models can better capture the topology of real cellular networks. However, the random cellular network models are often complicated to analyze. To overcome this gap, in this paper we propose to analyze the performance of PVT random cellular networks using Markov chains. Using this technique, the blocking probability and the area spectral efficiency (ASE) models are obtained. Numerical results are demonstrated which show that our proposed techniques are effective approaches to evaluate the performance of random cellular networks.

**Index Terms**—Markov chains; random cellular networks; blocking probability; spectrum efficiency

## I. INTRODUCTION

In the last decades, one-dimensional linear model and two-dimensional lattice model including square lattices and triangular lattices have been widely used for cellular network modeling and performance analysis [1]. However, the capacity demand is dynamically changing in different cell network areas. For example, residential and office areas need to be equipped more base stations (BSs) to provide high transmission capacity in cellular networks. Therefore, the regular deployment assumption in cellular network cannot capture the reality in BSs deployment. Ignoring these structural fluctuations of the BS deployments may cause significant bias on the evaluation of key system characteristics. As a consequence, the random cellular model is proposed to model the spatial structural fluctuations in real cellular networks [2]. Moreover, in many real scenarios, only a statistical description of the BS location is available which makes random cellular models suitable for describing these BSs deployment [3].

Win *et al.* investigated the aggregated interference distribution in cellular networks where interferers are scattered according to a spatial Poisson process [3]. Moreover, some critical factors, such as wireless propagation, transmission technology and spatial density of interfering nodes are analyzed assuming random interference models. Based on the assumption of Poisson BS deployments, modeling and performance analysis of heterogeneous cellular networks were studied in [4], [5]. Mukherjee calculated the probability of the user being able to

camp on a macrocell and an open-access femtocell in a three-tier network [4]. The probability was validated to be dependent on the relative densities and transmit powers of macrocell and femtocell, on the fraction of femtocell operating in open-access vs. closed subscriber group model and on wireless channel models. Based on a downlink heterogeneous cellular network consisting of  $K$  tiers of randomly located BSs, Dhillon *et al.* derived an expression for the probability of coverage over the entire network under both open and closed access schemes and obtained the average rate achieved by a typical mobile user [5]. The achievable transmission capacity of wireless backhaul mesh networks was explored in a two-tier network, where the spatial distribution of transmitters of the primary network is approximated by a Poisson point process and the node distribution of secondary network is relatively stationary [6]. Generally, it is complex to analyze the performance of cellular networks based on random cellular models.

On the other hand, the Markov chain model is a simple and efficient approach to describe wireless networks [7]–[12]. The most classical discrete channel model used for wireless networks is the Gilbert-Elliott channel model, where the state of the channel is marked as good or bad [7], [8]. Based on the Gilbert-Elliott channel model, the throughput and delay were analyzed for regular wireless networks [9], [10]. Based on a three-dimensional Markov chain, a pico-cellular airport traffic model was presented to evaluate the traffic congestion and call congestion for different types of traffic streams in [11]. A survey of the generalized finite-state Markov channel modeling of fading channels with its applications in wireless communication systems was presented in [12]. Nevertheless, there is little study on random cellular networks using Markov chain.

To overcome aforementioned gaps of Markov chain theory and random cellular theory in cellular network modeling, we try to combine the above two theories and build a new random cellular network model based on Markov chain. In this paper, we investigate the throughput and spectrum efficiency based on Markov chain for a Poisson-Voronoi tessellated (PVT) random cellular network. The main contributions of this paper are summarized as follows.

- 1) A random cellular network with Poissonly distributed BSs and PVT cell coverage is analyzed based on Markov chains.
- 2) Using the Markov chain model, the blocking probability and the area spectral efficiency (ASE) of the PVT cellular networks are analyzed.
- 3) The blocking probability and the ASE of PVT cellular networks are evaluated extensively using numerical simulations and on that basis some interesting observations are obtained.

The remainder of this paper is outlined as follows. Section II describes the system model. In Section III, a Markov chain model is proposed for modeling channel allocation in PVT random cellular networks. Based on the proposed Markov chain model, the blocking probability and the ASE are derived for PVT random cellular networks in Section IV. Moreover, the performance of the proposed models is analyzed by numerical simulations. Finally, Section V concludes this paper.

## II. SYSTEM MODEL

Assume that both mobile users (MUs) and BSs are located randomly in the infinite plane  $\mathbb{R}^2$ . Locations of MUs and BSs are assumed to be governed by two independent Poisson point processes, which are denoted as  $\Theta_U = \{x_i : i = 0, 1, 2, \dots\}$  and  $\Theta_B = \{y_j, j = 0, 1, 2, \dots\}$ , where  $x_i$  and  $y_j$  is the location of the  $i$ th MU  $MU_i$  and the  $j$ th BS  $BS_j$ , respectively. The intensities of the two Poisson point processes are  $\lambda_U$  and  $\lambda_B$ , respectively.

### A. Wireless Propagation Environments

The channel gain, defined as the ratio between the received power  $P_{r-x_i}$  at the MU  $x_i$  and the corresponding transmission power  $P_{y_j}$  from its associated BS  $y_j$  is

$$L_{y_j}(x_i) = \frac{P_{r-x_i}}{P_{y_j}} = \frac{K \cdot S_{y_j}(x_i)}{L(\|y_j - x_i\|)} = \frac{K \cdot S_{y_j}(x_i)}{\|y_j - x_i\|^b}, \quad (1)$$

where  $K$  is a constant depending on antenna gains; the term  $S_{y_j}(x_i)$  accounts for the fading and shadowing effects in wireless signal propagation environments;  $L(\|y_j - x_i\|)$  is the path loss between the receiving MU and the transmitting BS, which can be expressed as the function of distance  $\|y_j - x_i\|^b$  with path loss exponent  $b$  [13].

### B. User Association Scheme

In this paper, a MU  $x_i$  is assumed to associate with the closest BS  $y_j^*$ , which typically suffers the least path loss during wireless transmission. Therefore, the following requirement is satisfied

$$y_j^* = \arg \max_{y_j \in \Theta_B} \|y_j - x_i\|^{-b}. \quad (2)$$

Considering that the locations of MUs and BSs are governed by two independent Poisson point processes, the distance between two BSs is a random variable. As a consequence, the coverage of BS  $y_j$  is defined by

$$\mathcal{C}_{y_j} = \{y \in \mathbb{R}^2 : \|y - y_j\| \leq \|y - y_l\|, \forall y_l \in \Theta_B \text{ and } y_l \neq y_j\}. \quad (3)$$

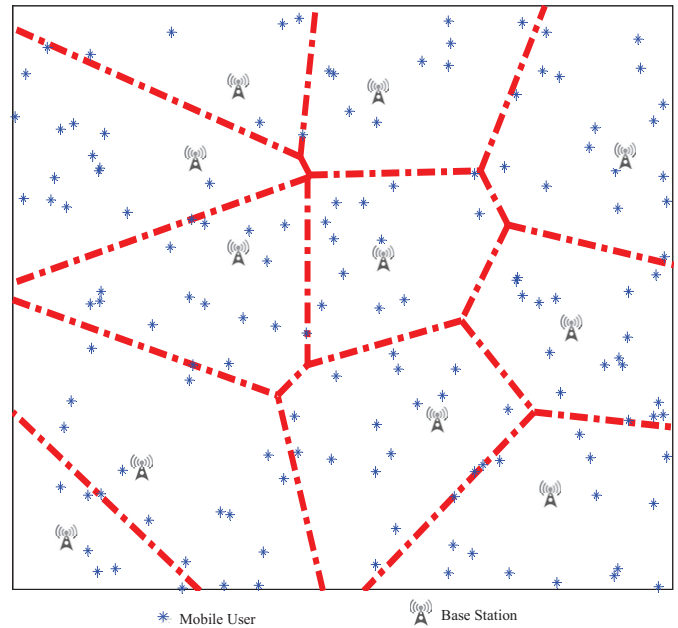


Fig. 1. Topology of PVT cellular network with  $\lambda_U = 0.2 (km)^{-2}$  and  $\lambda_B = 0.03 (km)^{-2}$ .

Based on (3), the topology of random cellular network is illustrated in Fig. 1. In Fig. 1, the polygons rounding by red dash lines are denoted as cells and the blue star points represent mobile users in cellular networks. This type of random cellular network is well known as the PVT cellular network. Based on the Palm theory and the Slivnyaks theorem [14], [15], the geometric characteristics of any cell coincide with that of a typical PVT cell where the BS is located at a fixed position. This feature implies that the analytical results for a typical PVT cell, such as the traffic load and the outage probability can be used to measure the performance of the whole PVT cellular network.

### C. Channel Allocation Scheme

A centralized channel allocation scheme is adopted in this paper. The MU is assumed to have all channel state information (CSI) in its cell. Considering the interference transmitted from adjacent cells, the signal-to-interference-and-noise ratio (SINR) is adopted to evaluate whether a channel is suitable for a MU with the specified QoS. A MU first measures all signal power over all unoccupied channels. If the value of SINR on a channel is large than or equal to a given threshold, this channel can be allocated for a MU and is marked as 1 in the channel table. If the value of SINR on a channel is less than a given threshold, this channel can not be allocated for a MU and is marked as 0 in the channel table. Furthermore, the MU submits the information of channel table to the associated BS. The BS collects all information of channel tables and forwards this information to the management center, which will coordinate channel allocation in adjacent cells to reduce interference on occupied channels. For example, when a MU  $x_i$  plans to occupy a channel  $c$  in the associated BS, the management

center will ensure that the SINR values of occupied channels with the same frequency band  $c$  in adjacent cells are large than or equal to the given threshold even if the new MU is added into cellular networks. In this way, we can avoid the situation that the currently occupied channels are interrupted by the new MU.

### III. MARKOV CHAIN MODEL AND OUTAGE PROBABILITY

#### A. Channel Allocation Markov Chain Model

Without loss of generality, a typical cell  $C_{ori}$  in the PVT cellular network is selected for Markov Chain modeling and performance analysis in this paper. In the typical cell  $C_{ori}$ , the call arriving to the system is assumed to follow a Poisson distribution with mean  $\lambda$ . The cell service time  $\mathcal{T}_S$  and the cell dwell time  $\mathcal{T}_D$  are assumed to be governed by exponential distributions with mean  $\mu$  and  $1/\mathcal{T}_D$ , respectively. The call holding time  $\mathcal{T}_H$  is defined as  $\mathcal{T}_H = \min(\mathcal{T}_S, \mathcal{T}_D)$ . Using the property of exponential distribution, the call holding time  $\mathcal{T}_H$  follows an exponential distribution with rate  $\eta = \mu + 1/\mathcal{T}_D$ . In this paper, the continuous Gilbert-Elliott channel model is used to model the transition between the available channels and the unavailable channels. The transition rate from the unavailable channel to the available channel is denoted as  $\alpha$ . The transition rate from the available channel to the unavailable channel is denoted as  $\beta$ .

The total number of channels in the cell  $C_{ori}$  is denoted as  $C$ . The channel state is related to the SINR value. Only when the SINR value of the channel is large than a given threshold  $\gamma_0$ , this channel can be allocated to a MU. Considering the interference from adjacent cells, SINR values of some channels are less than the given threshold  $\gamma_0$  in the cell  $C_{ori}$ . Therefore, the maximum number of channels that can be allocated for MUs is usually less than the total number of channels in the cell  $C_{ori}$ .

Let  $(m, n)$  be the system state vector, where  $m$  is the number of channels available to be allocated for MUs in the cell  $C_{ori}$ , and  $n$  is the number of occupied channels in the cell  $C_{ori}$ . Obviously,  $m$  is large than or equal to  $n$ . When the total number of channels in the cell  $C_{ori}$  is assumed to be 5, the corresponding Markov Chain transition diagram is illustrated in Fig. 2.

The Markov Chain state transition in Fig. 2 is described as follows:

- 1)  $(m, n) \rightarrow (m + 1, n)$ : When the instantaneous SINR value of an unavailable channel becomes large than or equal to the given threshold due to the time-varying interference caused by MU activities, the number of available channels is increased by 1.
- 2)  $(m, n) \rightarrow (m - 1, n)$ : When the instantaneous SINR value of an available channel becomes less than the given threshold due to the time-varying interference caused by MU activities, the number of available channels is decreased by 1.
- 3)  $(m, n) \rightarrow (m, n + 1)$ : When a new call arrives, the number of occupied channels is increased by 1 if the

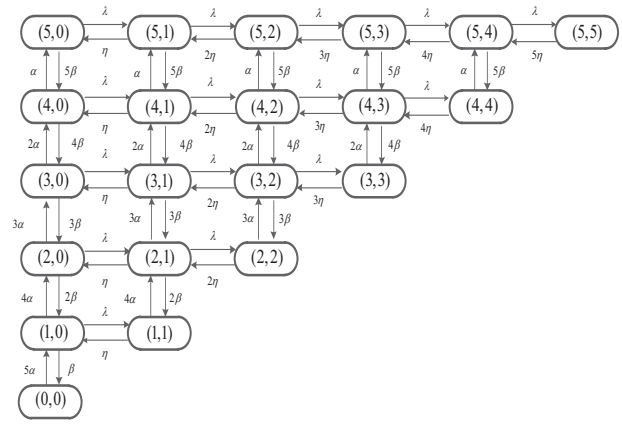


Fig. 2. Markov chain transition diagram with  $C = 5$ .

number of occupied channels is less than the number of available channels.

- 4)  $(m, n) \rightarrow (m, n - 1)$ : When a call has been successfully serviced, the number of occupied channels is decreased by 1 if this occupied channel is released.

Based on the Markov chain transition diagram in Fig. 2, the transition rate from the state  $S_h$  to the state  $S_k$ , denoted by  $\Lambda(S_h, S_k)$ , satisfies the following equality

$$\begin{aligned} & \Lambda(S_1, S_2) \cdot \Lambda(S_2, S_3) \cdot \dots \cdot \Lambda(S_{u-1}, S_u) \cdot \Lambda(S_u, S_1) \\ & = \Lambda(S_1, S_u) \cdot \Lambda(S_u, S_{u-1}) \cdot \dots \cdot \Lambda(S_3, S_2) \cdot \Lambda(S_2, S_1) \end{aligned} \quad (4)$$

Based on the Kolmogorovs criteria [16], Markov chain in Fig. 2 is reversible and the associated stationary state distribution exists. Thus, the global equilibrium equations are derived in (5). Based on (5), stationary state probabilities are expressed as  $\pi(m, n) = \chi \cdot \pi(m) \cdot \pi(n)$ , where  $\chi$  is a normalization factor,  $\pi(m)$  and  $\pi(n)$  are probabilities related to  $m$  and  $n$ , respectively. In detail, stationary state probabilities are derived as follows

$$\pi(m, n) = \begin{cases} \frac{1}{\chi} \left(\frac{\lambda}{\eta}\right)^n \frac{1}{n!} \binom{C}{m} \left(\frac{\alpha}{\beta}\right)^m \\ \chi = \sum_{n \leq m \leq C} \left(\frac{\lambda}{\eta}\right)^n \frac{1}{n!} \binom{C}{m} \left(\frac{\alpha}{\beta}\right)^m \end{cases} \quad (6)$$

#### B. $\alpha/\beta$ Ratio

The ratio between  $\alpha$  and  $\beta$  needs to be calculated in (6). Let  $\frac{\alpha}{\beta} = \frac{1-\varepsilon}{\varepsilon}$  and it is easy to derive  $\varepsilon$  by

$$\varepsilon = \frac{\beta}{\alpha + \beta}. \quad (7)$$

The probability of the unavailable channel is defined as  $\frac{\beta}{\alpha + \beta}$  in Gilbert-Elliott channel models. Referring to the definition of the unavailable channel in Gilbert-Elliott channel models,  $\varepsilon$  is also the probability of the unavailable channel. In this paper, the channel is unavailable when the SINR value of channel is less than the given threshold. In this case, the probability of unavailable channel is equal to the outage probability.

$$\begin{cases}
 C\alpha\pi(0,0) = \beta\pi(1,0) \\
 [m\beta + \lambda + (C-m)\alpha]\pi(m,0) = (C-m+1)\alpha\pi(m-1,0) + \eta\pi(m,1) + (m+1)\beta\pi(m+1,0) \quad \text{for } 0 < m < C \\
 [C\beta + \lambda]\pi(C,0) = \alpha\pi(C-1,0) + \eta\pi(C,0) \\
 [C\beta + \lambda + n\eta]\pi(C,j) = \alpha\pi(C-1,n) + (n+1)\eta\pi(C,n+1) + \lambda\pi(C,n-1) \quad \text{for } 0 < n < C \\
 C\eta\pi(C,C) = \lambda\pi(C,C-1) \\
 [(C-m)\alpha + i\eta]\pi(m,m) = \lambda\pi(m,m-1) + (i+1)\beta\pi(m+1,j) \quad \text{for } 0 < n = m < C \\
 [m\beta + (C-m)\alpha + \lambda + n\eta]\pi(m,n) = (C+1-m)\alpha\pi(m-1,n) + (m+1)\beta\pi(m+1,n) + (m+1)\eta\pi(m,n+1) \\
 + \lambda\pi(m,n-1) \quad \text{for } 0 < n < m < C
 \end{cases} \quad (5)$$

Considering that infinite interference transmitters are scattered in an infinite plane, the outage probability  $\varepsilon$  is expressed as

$$\varepsilon = p_{out} = P(SINR_{y_j}(x_i) < \gamma_0 | x_i \in \mathcal{C}_{ori}), \quad (8a)$$

with

$$\begin{aligned}
 SINR_{y_j}(x_i) &= \frac{S}{W+I} \\
 &= \frac{P_{y_l} \cdot K \cdot S_{y_j}(x_i) \{L(\|y_l - x_i\|)\}^{-1}}{\sigma^2 + I_{x_i}} \quad (8b)
 \end{aligned}$$

$$I_{x_i} = \sum_{y_l \in \Theta_B \setminus \{y_j\}} P_{y_l} \cdot K \cdot S_{y_l}(x_i) \{L(\|y_l - x_i\|)\}^{-1}, \quad (8c)$$

where  $I_{x_i}$  is the aggregated interference received by a mobile user located at  $x_i$ ,  $\sigma^2$  is the constant Gaussian additive noise power.

The success probability was derived for a randomly located mobile user where signals experience a fading distribution [17]. The user is assumed to be associated with the closest BS and  $S_{y_j}(x_i)$  is assumed to follow a Rayleigh distribution. To simplify the derivation, we assume  $S_{y_j}(x_i) \sim \exp(1)$ . Based on results in [17], we derive a user success probability where desired signals and interference are governed by a Rayleigh distribution, which is expressed by

$$p_{suc} = \pi\lambda_B \int_0^{+\infty} e^{-\pi\lambda_B s(1+\kappa) - \gamma_0 \sigma^2 s^{b/2} / P_{y_j} \cdot K} ds, \quad (9a)$$

with

$$\kappa = \gamma_0^{2/b} \int_{\gamma_0^{-2/b}}^{+\infty} \frac{1}{1+v^{b/2}} dv. \quad (9b)$$

The outage probability is derived by

$$\begin{aligned}
 p_{out} &= 1 - p_{suc} \\
 &= 1 - \pi\lambda_B \int_0^{+\infty} e^{-\pi\lambda_B s(1+\kappa) - \gamma_0 \sigma^2 s^{b/2} / P_{y_j} \cdot K} ds \quad (10)
 \end{aligned}$$

## IV. PERFORMANCE ANALYSIS AND NUMERICAL RESULTS

### A. Performance Analysis

In the proposed system model, a call will be blocked if the number of active mobile users exceeds that of available channels in a cell. Obviously, the number of available channels is time-varying due to interference. Since no buffer is considered

in our proposed system model, the call blocking probability is defined as

$$\begin{aligned}
 p_b &= \sum_{m=n \leq C} \pi(m,n) \\
 &= \sum_{m=n \leq C} \frac{1}{\lambda} \left(\frac{\lambda}{\eta}\right)^m \frac{1}{m!} \binom{C}{n} \left(\frac{\alpha}{\beta}\right)^n \quad (11)
 \end{aligned}$$

Based on (11), the blocking probability is determined by the limited availability of channel or spectrum resource as well as time-varying characteristic of channel itself.

The bandwidth of a typical cell  $\mathcal{C}_{ori}$  is assumed to be  $B$ . According to the Shannon channel capacity, the throughput of a typical cell is derived by

$$\begin{aligned}
 T_{throughput} &= (1 - p_b) B \cdot E[\log_2(1 + SINR_{y_j}(x_i))] \\
 &\quad \cdot \sum_{0 \leq m \leq n \leq C} m \cdot \pi(m,n) \quad (12)
 \end{aligned}$$

In (12), the link capacity between a single mobile user and an associated BS is

$$\begin{aligned}
 &E[\log_2(1 + SINR_{y_j}(x_i))] \\
 &= \int_0^{+\infty} P(\log_2(1 + SINR_{y_j}(x_i)) > t) dt \\
 &= \int_0^{+\infty} P(SINR_{y_j}(x_i) > 2^t - 1) dt \\
 &= \pi\lambda_B \int_0^{+\infty} \int_0^{+\infty} e^{-\pi\lambda_B s(1+\kappa') - (2^t - 1)\sigma^2 s^{b/2} / P_{y_j} \cdot K} ds dt \quad (13a)
 \end{aligned}$$

with

$$\kappa' = (2^t - 1)^{2/b} \int_{(2^t - 1)^{-2/b}}^{+\infty} \frac{1}{1+v^{b/2}} dv. \quad (13b)$$

(13a) is derived based on the relationship between the expectation and cumulative distribution function (CDF) of a random variable. A simple proof is given as follows. For a random variable  $x$  with continuous probability distribution function (PDF), its expectation is expressed by  $E(x) = \int_{-\infty}^{+\infty} x f(x) dx = \int_{-\infty}^0 x f(x) dx + \int_0^{+\infty} x f(x) dx$ . The first and second terms of the expression are rewritten below.

$$\begin{aligned}
 \int_{-\infty}^0 x f(x) dx &= - \int_{-\infty}^0 \left( \int_x^0 dy \right) f(x) dx \\
 &= - \int_{-\infty}^0 \int_{-\infty}^y f(x) dx dy \quad (14a) \\
 &= - \int_{-\infty}^0 F(y) dy
 \end{aligned}$$

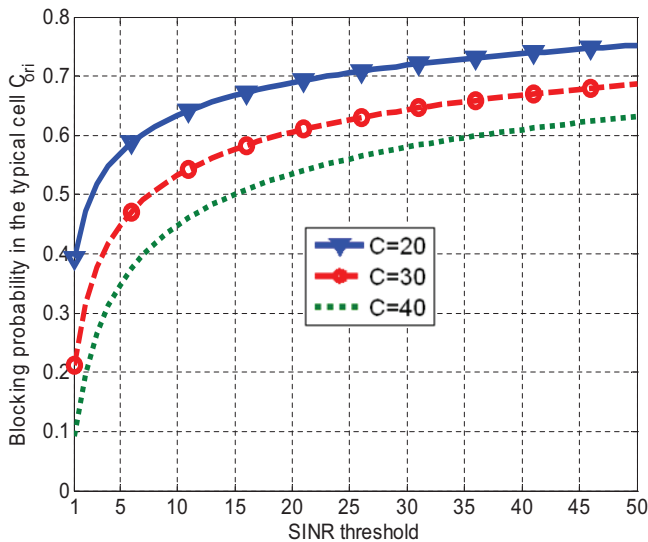


Fig. 3. Blocking probability with respect to the SINR threshold considering different channel numbers in the cell  $C_{ori}$ .

$$\begin{aligned} \int_0^{+\infty} x f(x) dx &= \int_0^{+\infty} \left( \int_0^x dy \right) f(x) dx \\ &= \int_0^{+\infty} \int_y^{+\infty} f(x) dx dy, \quad (14b) \\ &= \int_0^{+\infty} [1 - F(y)] dy \end{aligned}$$

where  $F(\cdot)$  is CDF. As we all know,  $SINR_{y_j}(x_i) \geq 0$ . Thus, the integration of (14a) is zero and (13a) is obtained. Using the Palm theory and the Slivnyaks theorem, the spatial characteristics of any PVT cells is coincided with that of the typical PVT cell  $C_{ori}$ .

Furthermore, the ASE of the entire system is defined by [18]

$$ASE = \lambda_B \cdot T_{throughput}. \quad (15)$$

### B. Numerical Results

To analyze the performance of our proposed models, some default parameters are listed in Table I for numerical simulations.

TABLE I  
PARAMETER VALUES USED IN NUMERICAL SECTION

Parameter	Value
$\lambda_B$	$0.2(km)^{-2}$
$C$	20
$B$	0.1MHz
$\lambda$	$1min^{-1}$
$\mu$	$0.05min^{-1}$
$T_D$	20min
$P_{y_j}$	30dBm
$\sigma^2$	0dBm
$b$	4
$K$	31.54dB

Fig. 3 shows the call blocking probability with respect to the SINR threshold which varies from 1 to 50 considering different channel numbers  $C$  in the cell  $C_{ori}$ . When the channel number is fixed in the cell  $C_{ori}$ , it is observed that the

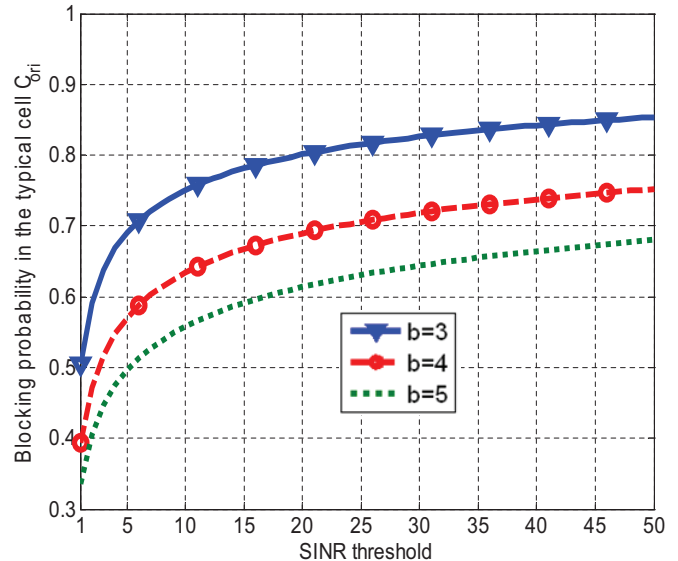


Fig. 4. Blocking probability with respect to the SINR threshold considering different path loss exponents in the cell  $C_{ori}$ .

call blocking probability increases with the increasing SINR threshold, but the growth rate decreases. The reason is that the successful receiving signal is decreased at terminals when the SINR threshold is larger. When the SINR threshold is fixed, the call blocking probability increases with the decreasing channel number in the cell  $C_{ori}$ .

Fig. 4 illustrates the call blocking probability versus the SINR threshold for different path loss  $b$  in the cell  $C_{ori}$ . When the SINR threshold is fixed, the call blocking probability decreases with the increase of path loss exponents. We know that the path loss coefficient affects both desired signal and interference signals. However, these curves imply that path loss coefficient has a more significant impact on the aggregated interference.

The ASE with respect to the SINR threshold considering different BS intensities is plotted in Fig. 5. The ASE decreases with the increasing SINR threshold when the BS intensity is a fixed value. This is because spectrum resources can not be fully utilized due to the high blocking probability when the SINR threshold is large. When we fix the SINR threshold, the ASE increases with the increasing of BS intensity. Higher BS intensity means smaller cell size and shorter signal propagation distance. Thus, a conclusion is drawn that the reduction of the cell size will increase the ASE.

Fig. 6 compares the ASE with respect to the SINR threshold considering different call arrival rates in the cell  $C_{ori}$ . When we fix the SINR threshold, ASE decreases with the increasing of call arrival rate.

### V. CONCLUSION

Based on Markov chains, a new PVT random cellular network model is proposed. The blocking probability and the ASE are derived to evaluate the PVT random cellular networks. To achieve these models, a Markov chain model

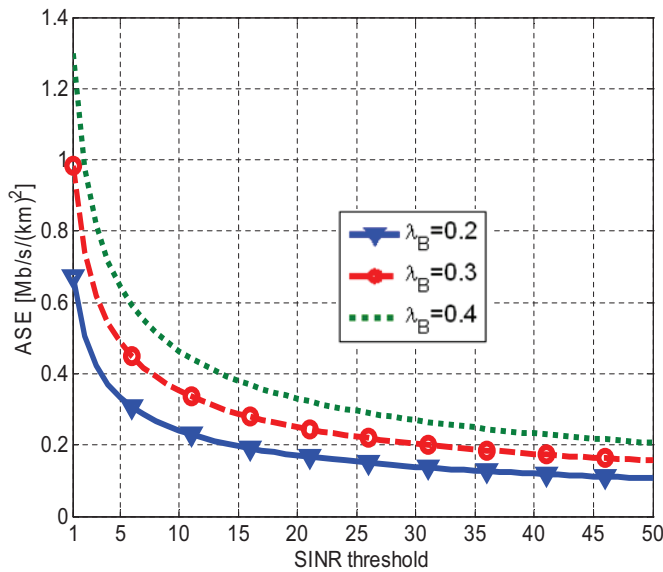


Fig. 5. ASE with respect to the SINR threshold considering different BS intensities in the cell  $C_{ori}$ .

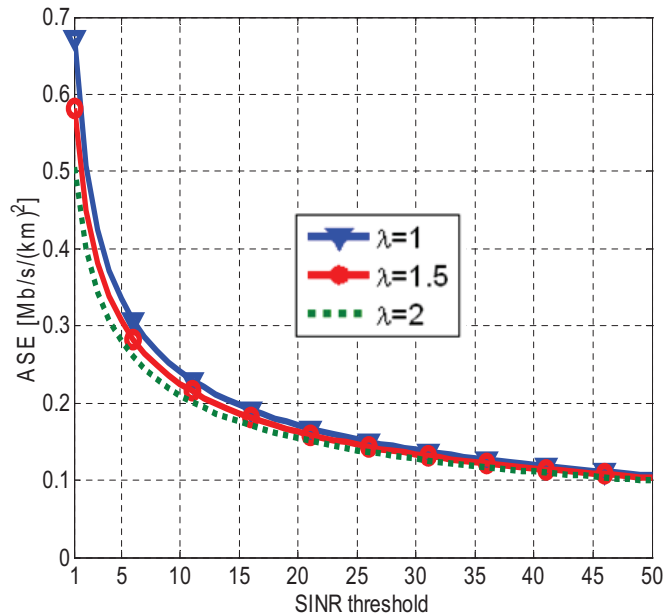


Fig. 6. ASE with respect to the SINR threshold considering different call arrival rates in the cell  $C_{ori}$ .

is presented for the PVT random cellular networks. Moreover, performance of PVT random cellular networks is analyzed using numerical results. By combining the PVT random theory and Markov chain theory, we find a new approach to model the cellular networks. Our results provide insights into the radio resource (e.g., wireless channels) optimization in PVT cellular networks

#### ACKNOWLEDGMENT

The authors would like to acknowledge the support from the International Science and Technology Cooperation Program

of China under the grants 2014DFA11640 and 0903, National Natural Science Foundation of China (NSFC) under the grants 61271224 and 61301128, NFSC Major International Joint Research Project under the grant 61210002, the Hubei Provincial Science and Technology Department under the grant 2013B-HE005, the Fundamental Research Funds for the Central Universities under the grant 2011QN020 and 2013QN136, and Special Research Fund for the Doctoral Program of Higher Education (SRFDP) under the grant 20130142120044. This research is partially supported by EU FP7-PEOPLE-IRSES, project acronym S2EuNet (grant no. 247083), project acronym WiNDOW (grant no. 318992) and project acronym CROWN (grant no. 610524). Guoqiang Mao's work is supported by Australian Research Council Discovery projects DP110100538 and DP120102030.

#### REFERENCES

- [1] W. C. Y. Lee, "Elements of cellular mobile radio systems," *IEEE Trans. Veh. Technol.*, vol. 35, no. 2, pp. 48–56, May 1986.
- [2] F. Baccelli, M. Klein, M. Lebourges, and S. Zuyev, "Stochastic geometry and architecture of communication networks," *J. Telecommunication Systems*, 1997.
- [3] M. Win, P. Pinto, and L. Shepp, "A mathematical theory of network interference and its applications," in *Proc. of the IEEE*, vol. 97, no. 2, pp. 205–230, Feb. 2009.
- [4] S. Mukherjee, "Distribution of downlink SINR in heterogeneous cellular networks," *IEEE J. Sel. Areas Commun.*, vol. 30, no. 3, pp.575–585, April 2012.
- [5] H. S. Dhillon, R. K. Ganti, F. Baccelli, and J. G. Andrews, "Modeling and analysis of k-tier downlink heterogeneous cellular networks," *IEEE J. Sel. Areas Commun.*, vol. 30, no. 3, pp. 550–560, April 2012.
- [6] T. Jing, X. Chen, Y. Huo, and X. Cheng, "Achievable transmission capacity of cognitive mesh networks with different media access control," in *Proc. of IEEE INFOCOM*, March 2012.
- [7] E. N. Gilbert, "Capacity of a burst-noise channel," *Bell Syst. Tech. J.*, vol. 39, no. 9, pp. 1253–1265, Sep. 1960.
- [8] E. O. Elliott, "Estimates of error rates for codes on burst-noise channels," *Bell Syst. Tech. J.*, vol. 42, no. 9, pp. 1977–1997, Sep. 1963.
- [9] R. Jayaparvathy, S. Anand, and S. Srikanth, "Performance analysis of dynamic packet assignment in cellular systems with OFDMA," in *Proc. of the IEEE*, vol. 152, no.1, pp. 45–52, Feb. 2005.
- [10] S. Anand, A. Sridharan, and K. N. Sivarajan, "Performance analysis of channelized cellular systems with dynamic channel allocation," *IEEE Trans. Veh. Technol.*, vol. 52, no. 4, pp. 847–859, July 2003.
- [11] S. Bhattacharya, B. R. Qazi, and J. M. H. Elmirghani, "A 3-D Markov chain model for a multi-dimensional indoor environment," in *Proc. of IEEE GLOBECOM 2010*, Dec. 2010.
- [12] P. Sadeghi, R. A. Kennedy, P. B. Rapajic, and R. Shams, "Finite-state Markov modeling of fading channels – a survey of principles and applications," *IEEE Signal Process. Mag.*, vol. 25, no. 5, pp. 57–80, Sep. 2008.
- [13] T. S. Rappaport, *Wireless Communications: Principles and Practice*. Englewood Cliffs, NJ: Prentice-Hall, 1996.
- [14] L. Xiang, X. Ge, C.-X. Wang, F. Y. Li, and F. Reichert, "Energy efficiency evaluation of cellular networks based on spatial distributions of traffic load and power consumption," *IEEE Trans. Wireless Commun.*, vol. 12, no. 3, pp. 961–973, March 2013.
- [15] D. Stoyan, W. S. Kendall, and J. Mecke, *Stochastic Geometry and Its Applications*, 2nd edition. Wiley, 1996.
- [16] F. P. Kelly, *Reversibility and Stochastic Network*. Wiley, 1979.
- [17] J. G. Andrews, F. Baccelli, and R. K. Ganti, "A tractable approach to coverage and rate in cellular networks," *IEEE Trans. Commun.*, vol. 59, no. 11, pp. 3122–3134, Nov. 2011.
- [18] Y. Soh, T. Quek, M. Kountouris, and H. Shin, "Energy efficient heterogeneous cellular networks," *IEEE J. Sel. Areas Commun.*, vol. 31, no. 5, pp. 840–850, May 2013.